Journal of Applied Mechanics and Technical Physics, Vol. 47, No. 2, pp. 254–265, 2006

DYNAMIC DEFORMATION OF A CURVED PLATE WITH A RIGID INSERT

Yu. V. Nemirovsky and T. P. Romanova

UDC 539.4+539.37

A general solution is obtained for dynamic bending of ideal rigid-plastic plates with a clamped or simply supported curved contour containing an absolutely rigid insert of an arbitrary shape. The plate is affected by a short-time high-intensity explosive dynamic load uniformly distributed over the surface. It is shown that there are several mechanisms of plate deformation. Equations for dynamic deformation are derived for each mechanism, and conditions of occurrence are analyzed. Examples of numerical solutions are given.

Key words: *rigid-plastic plate, arbitrary contour, rigid insert, dynamic load, ultimate load, final flexure.*

Introduction. The issues of calculating structures under the action of intense short-time loads are very important in modern mechanics of deformable solids. To solve such problems, the model of a rigid-plastic body is widely used [1]. The model is based on the assumption that the body starts deforming when the stress reaches the ultimate value and plastic deformation becomes possible. Elastic deformations are neglected. For thin-sheet structural elements, this simplification allowed solving numerous issues of practical importance. The model of a rigid-plastic body was used in [2–9] to study the behavior of homogeneous plates with a complicated external contour under the action of arbitrary dynamic loads of high intensity.

Structurally inhomogeneous plates are constitutive elements of many structures used in various areas of engineering. Flat shields are often equipped by reinforced closed technological hatches. Therefore, damage of plates with rigid inserts has to be examined. Up to now, this problem has been considered only for a circular plate with a rigid circle at the center under conditions of axisymmetric loading and attachment [10]. The method proposed in the present work allows, on the basis of the theory of an ideal rigid-plastic body, calculating plates with an arbitrary curved contour, which are attached in an arbitrary manner, have an absolutely rigid insert of an arbitrary shape, and are subjected to intense short-time dynamic loads. The method can be used for a wide class of approximate engineering calculations.

1. We consider a plate made of an ideal rigid-plastic material with an arbitrary smooth convex contour l, which is clamped or simply supported (Fig. 1). In the central part, the plate has an absolutely rigid insert Z_a with an arbitrary contour l_2. The plate is subjected to a high-intensity dynamic load $P(t)$ uniformly distributed over the surface. We consider explosive loads characterized by instantaneous reaching the maximum value $P_{\max} = P(t_0)$ at the initial time t_0 with their subsequent rapid decrease. As the insert Z_a remains rigid during its deformation, we assume that the ultimate flexural moment in the insert is greater than M_0 (the ultimate flexural moment in the remaining part of the plate) and $\rho_a/\rho \geqslant 1$, where ρ and ρ_a are the surface densities of the plate and insert materials, respectively.

The dynamics of the plate made of a rigid-plastic material can follow one of the three schemes of deformation, depending on the value of $P_{\max}$. Under loads lower than the ultimate values (low loads), the plate remains at rest. Under loads only slightly higher than the ultimate values (medium loads), the plate is deformed into a certain line

Institute of Theoretical and Applied Mechanics, Siberian Division, Russian Academy of Sciences, Novosibirsk 630090; nemirov@itam.nsc.ru. Translated from Prikladnaya Mekhanika i Tekhnicheskaya Fizika, Vol. 47, No. 2, pp. 126–138, March–April, 2006. Original article submitted May 23, 2005.

 0021-8944/06/4702-0254 © 2006 Springer Science + Business Media, Inc.

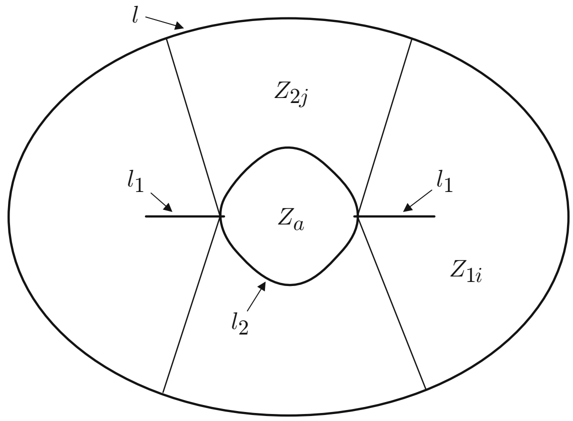

Fig. 1

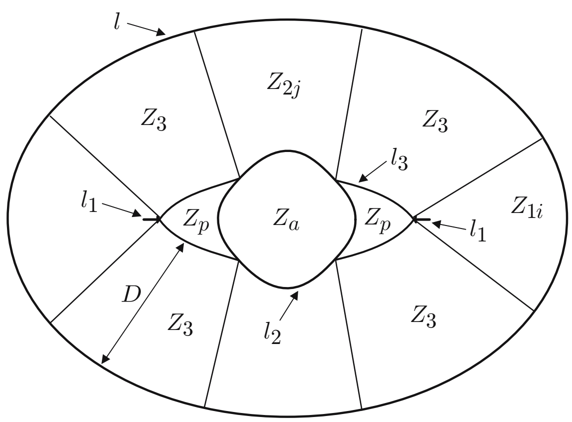

Fig. 2

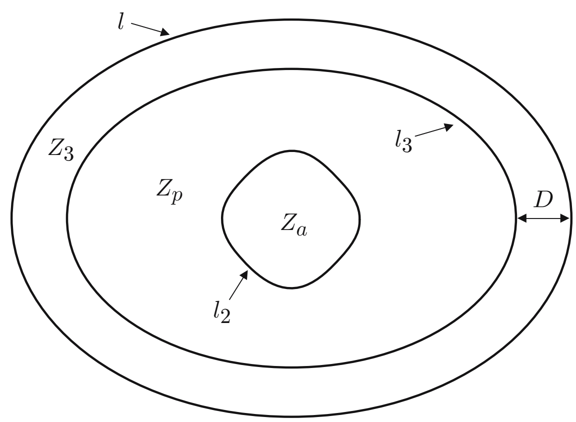

Fig. 3

surface, whereas the absolutely rigid insert and the points of its contour move translationally with an identical velocity $\dot{w}_c(t)$. As in the case of a plate without the insert [4, 6–9], a plastic pivot line l_1 can be formed in the plate; this line may consist of several segments (see Fig. 1). The position of the line l_1 is determined by the shape of the support contour of the plate from the condition of identical distances from the contour l to the line l_1 in the direction normal to the external contour [7, 9]. This scheme of deformation is called scheme No. 1. As in the case of flexure of beams [1], circular and annular plates [12–14], rectangular and polygonal plates [1–3, 11], and plates with a sophisticated contour [4–9], the plate dynamics in the case of rather high values of $P_{\max}$ can be accompanied by the emergence of a zone of intense plastic deformation Z_p moving translationally. There are also possible situations where some part of the pivot l_1 is retained or the zone Z_p does not cover the entire insert Z_a (high loads; scheme in Fig. 2 is called scheme No. 2) or where the pivot l_1 is absent and the insert Z_a is inside the zone Z_p (superhigh loads; scheme in Fig. 3 is called scheme No. 3).

Let the equation for the plate contour l be set in a parametric form: $x = x_1(\varphi)$ and $y = y_1(\varphi)$ $(0 \leqslant \varphi \leqslant 2\pi)$. In all schemes of deformation, the normal to the curve l directed inward the region occupied by the plate hits the pivot l_1, the contour l_2, or the curve l_3, which is the contour of the zone Z_p (see Figs. 1–3). We use the notation Z_{ij} to denote the zone of the plate, the normal from each point of this zone to the contour l being incident onto the curve l_i $(i = 1, 2, 3;\ j = 1, \ldots)$. The number of the curves l_i depends on the shapes of the plate and the insert. We denote part of the external contour l_{ij}, which is the support contour of the zone Z_{ij}, by l_{ij}. Part of the contour l_{ij} is determined in the interval $\psi_{ij} \leqslant \varphi \leqslant \xi_{ij}$ $(i = 1, 2, 3;\ j = 1, \ldots)$. We use the notation D_{nj} to denote the distance normal to the contour l, calculated from the contour l_{nj} to the curve l_n in the zone Z_{nj} $(n = 1, 2)$. The values of D_{nj} depend on the shapes of the plate and insert contours, hence, on the parameter φ only. It can be shown

[4, 6] that the normal to the contour l is also the normal to the curve l_3 and that the distance D between l_{3j} and l_3 is independent of the parameter φ and the subscript j. The equation l_3 [$x = x_3(\varphi)$ and $y = y_3(\varphi)$, where $\psi_{3j} \leqslant \varphi \leqslant \xi_{3j}$] for the contour of the zone Z_p has the form [4, 6]

$$x_3 = x_1 - Dy_1'/L, \qquad y_3 = y_1 + Dx_1'/L. \tag{1}$$

Here $L(\varphi) = \sqrt{x_1'^2(\varphi) + y_1'^2(\varphi)}$, where $(\,\cdot\,)' = \partial(\,\cdot\,)/\partial\varphi$.

We derive the equations of plate motion from the principle of virtual powers with the use of the d'Alembert principle [11]:

$$K = A - N; \tag{2}$$

$$K = \iint\limits_{S\setminus Z_a} \rho\, \frac{\partial^2 u}{\partial t^2}\, \frac{\partial u^*}{\partial t}\, ds + \iint\limits_{Z_a} \rho_a\, \frac{\partial^2 u}{\partial t^2}\, \frac{\partial u^*}{\partial t}\, ds,$$
$$A = \iint\limits_{S} P(t)\, \frac{\partial u^*}{\partial t}\, ds, \qquad N = \sum_m \int\limits_{l_m} M_m \Big[\frac{\partial \theta_m^*}{\partial t}\Big]\, dl. \tag{3}$$

Here K, A, and N are the powers of inertial, external, and internal forces of the plate, respectively, S is the plate area, u is the flexure, t is the current time, l_m are the lines of discontinuity of angular velocities, M_m is the flexural moment on l_m, and $[\partial\theta_m^*/\partial t]$ is the discontinuity of angular velocity on l_m. In the expression for N, summation is performed over all lines of discontinuity of angular velocity, including the plate boundary. Admissible velocities are indicated by the asterisk.

As the zones Z_a and Z_p move translationally, the flexural velocity in the zone Z_p is $\dot w_c(t)$ because of continuity of velocities at the boundaries of these zones. We denote the velocities of the angle of deflection of the zone Z_{ij} on the support contour l_{ij} by $\dot\alpha_{ij}$ ($i = 1, 2, 3$; $j = 1, \ldots$). The condition of continuity of velocities at the boundaries of the zones Z_{3j} and Z_p yields $\dot w_c = \dot\alpha_{3j} D$; hence, $\dot\alpha_{3j}$ is independent of the parameter φ and the subscript j. We denote $\dot\alpha_{3j}$ by $\dot\alpha$. Then, the flexural velocities in different zones of the plate can be presented as

$$(x, y) \in Z_a\colon \quad \dot u(x, y, t) = \dot w_c(t), \qquad (x, y) \in Z_p\colon \quad \dot u(x, y, t) = \dot w_c(t),$$
$$(x, y) \in Z_{3j}\colon \qquad \dot u(x, y, t) = \dot\alpha(t) d_{3j}(x, y) \quad (j = 1, \ldots), \tag{4}$$
$$(x, y) \in Z_{nm}\colon \qquad \dot u(x, y, t) = \dot\alpha_{nm}(t, \varphi) d_{nm}(x, y) \quad (n = 1, 2;\ m = 1, \ldots),$$

where $d_{ij}(x, y)$ is the distance from the point (x, y) to the support contour of the zone Z_{ij} ($i = 1, 2, 3$; $j = 1, \ldots$), and the dot over the symbols indicates their derivatives with respect to time.

As in [9], we assume that $\dot\alpha_{1j}$ is independent of the parameter φ but may depend on the subscript j. From the condition of continuity of velocities at the boundaries of the contacting zones [Z_{1i} and Z_{2j}; Z_{3m} and Z_{kn} ($i, j, m, n, = 1, \ldots$; $k = 1, 2$)], we obtain the relations

$$\dot\alpha_{1i}(t) D_{1i}(\varphi_*) = [\dot\alpha_{2j}(t, \varphi_*) D_{2j}(\varphi_*)]^{\mu_{ij}} (\dot\alpha D)^{\lambda_{1i}}; \tag{5}$$

$$\dot\alpha_{2n}(t, \varphi_{**}) D_{2n}(\varphi_{**}) = [\dot\alpha_{1m}(t) D_{1m}(\varphi_{**})]^{\mu_{mn}} (\dot\alpha D)^{\lambda_{2n}}, \tag{6}$$

where φ_* and φ_{**} are the parameters of the zone boundaries considered; $\mu_{ij} = 1$ if the zones Z_{1i} and Z_{2j} are in contact and $\mu_{ij} = 0$ if the zones Z_{1i} and Z_{2j} do not contact each other; $\lambda_{kj} = 1$ if the zones Z_{3i} and Z_{kj} are in contact and $\lambda_{kj} = 0$ if the zones Z_{3i} and Z_{kj} do not contact each other. It follows from equalities (5) and (6) that

$$\dot\alpha_{ij}(t, \varphi) = F_{ij}(t, \varphi)\dot\alpha(t) \qquad (i = 1, 2; \quad j = 1, \ldots). \tag{7}$$

The power of the internal forces in Eq. (3) is calculated by the formula (see [15])

$$N = M_0(2 - \eta) \oint\limits_{l} \frac{\partial \dot u^*}{\partial n}\, dl,$$

where $\eta = 0$ if the external contour is clamped and $\eta = 1$ if the external contour is simply supported; $\partial\dot u/\partial n$ is the derivative of the flexural velocity along the normal to the contour l or the velocity of the angle of deflection of the plate surface from the horizontal line on the contour l; dl is an element of the contour l.

With allowance for the notation used and for the equality $F_{3j} = 1$, Eqs. (3) become

$$K = \dot{\alpha}^* \ddot{\alpha} \rho \sum_{i,j} \iint\limits_{Z_{ij}} F_{ij}^2 d_{ij}^2 \, ds + \dot{w}_c^* \ddot{w}_c \Big[\rho \iint\limits_{Z_p} ds + \rho_a \iint\limits_{Z_a} ds \Big],$$

$$A = P(t) \Big[\dot{\alpha}^* \sum_{i,j} \iint\limits_{Z_{ij}} F_{ij} d_{ij} \, ds + \dot{w}_c^* \iint\limits_{Z_a \cup Z_p} ds \Big], \qquad N = M_0(2-\eta) \dot{\alpha}^* \sum_{i,j} \int\limits_{l_{ij}} F_{ij} \, dl.$$

Substituting these equalities into (2) and taking into account that $\dot{w}_c^*(t)$ and $\dot{\alpha}^*(t)$ are independent of each other, we obtain the equations of motion for the deformation scheme No. 2:

$$\rho \ddot{\alpha} \sum_{i,j} \iint\limits_{Z_{ij}} F_{ij}^2 d_{ij}^2 \, ds = P(t) \sum_{i,j} \iint\limits_{Z_{ij}} F_{ij} d_{ij} \, ds - M_0(2-\eta) \sum_{i,j} \int\limits_{l_{ij}} F_{ij} \, dl; \tag{8}$$

$$\ddot{w}_c \Big[\rho \iint\limits_{Z_p} ds + \rho_a \iint\limits_{Z_a} ds \Big] = P(t) \iint\limits_{Z_a \cup Z_p} ds. \tag{9}$$

The condition of continuity of velocities at the boundaries of the zones S_p and Z_{3j} yields the equality

$$\dot{\alpha} D = \dot{w}_c. \tag{10}$$

At the boundaries of the contacting zones Z_{ij} and Z_{mn} $(i, m = 1, 2)$, the following condition is satisfied:

$$D_{ij}(\beta_{ijmn}) = D_{mn}(\beta_{ijmn}). \tag{11}$$

Here the parameter β_{ijmn} determines the boundary of the zones Z_{ij} and Z_{mn} ($\beta_{ijmn} = \psi_{ij}$ or $\beta_{ijmn} = \xi_{ij}$).

The boundaries of the zones Z_{ij} $(i = 1, 2)$ and Z_{3n} obey the equality

$$D = D_{ij}(\varphi_{ij}), \tag{12}$$

where $\varphi_{ij} = \psi_{ij}$ or $\varphi_{ij} = \xi_{ij}$.

At the initial time, the plate is at rest, i.e.,

$$\alpha(t_0) = \dot{\alpha}(t_0) = w_c(t_0) = \dot{w}_c(t_0) = 0. \tag{13}$$

The initial values of $D(t_0)$ and $\beta_{ijmn}(t_0)$ are determined depending on the value of $P_{\max}$, which will be demonstrated below for particular problems.

System (7)–(12) describes the plate motion for the case of deformation by scheme No. 2. In the case of deformation by scheme No. 3, there are no zones Z_{1i} and Z_{2j}, the zones Z_{3n} merge into one zone, and the motion is described by Eqs. (8)–(10) with $i = 3$.

In the case of deformation by scheme No. 1, there are no zones Z_{3n}; the equalities

$$\dot{\alpha}_{ij}(t, \varphi) = G_{ij} \dot{w}_c(t), \quad G_{1j} = \frac{1}{D_{1j}(\varphi_*)}, \quad G_{2j}(\varphi) = \frac{1}{D_{2j}(\varphi)} \quad (i = 1, 2;\ j = 1, \ldots) \tag{14}$$

are valid instead of Eqs. (7) and (1) and expressions (3) acquire the form

$$K = \dot{w}_c^* \ddot{w}_c \Big(\rho \sum_{i=1,2} \sum_j \iint\limits_{Z_{ij}} G_{ij}^2 d_{ij}^2 \, ds + \rho_a \iint\limits_{Z_a} ds \Big),$$

$$A = \dot{w}_c^* P(t) \Big(\sum_{i=1,2} \sum_j \iint\limits_{Z_{ij}} G_{ij} d_{ij} \, ds + \iint\limits_{Z_a} ds \Big), \qquad N = \dot{w}_c^* M_0(2-\eta) \sum_{i=1,2} \sum_j \int\limits_{l_{ij}} G_{ij} \, dl.$$

Substituting these equalities into Eq. (2), we obtain

$$\ddot{w}_c \Big(\rho \sum_{i=1,2} \sum_j \iint\limits_{Z_{ij}} G_{ij}^2 d_{ij}^2 \, ds + \rho_a \iint\limits_{Z_a} ds \Big)$$

$$= P(t) \Big(\sum_{i=1,2} \sum_j \iint\limits_{Z_{ij}} G_{ij} d_{ij} \, ds + \iint\limits_{Z_a} ds \Big) - M_0(2-\eta) \sum_{i=1,2} \sum_j \int\limits_{l_{ij}} G_{ij} \, dl. \tag{15}$$

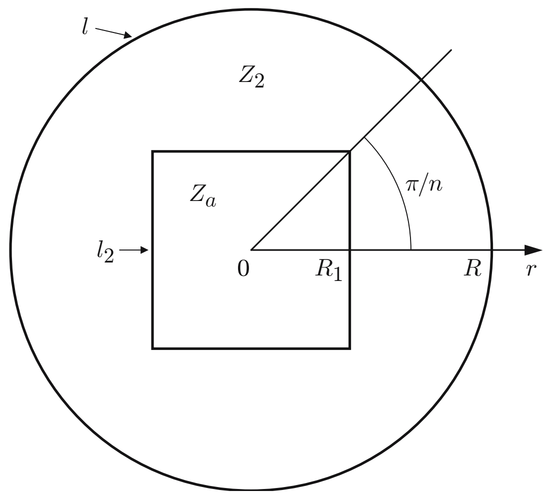

Fig. 4

System (14), (15) describes the plate motion for the case of deformation by scheme No. 1. Deflections in different zones of the plate are determined by Eqs. (4).

To calculate double integrals over the zones Z_{ij} ($i = 1, 2, 3$; $j = 1, \ldots$) in the equations of motion, it is convenient to pass to a curvilinear coordinate system (ν_1, ν_2) related to the Cartesian coordinate system as

$$x = x_1(\nu_2) - \nu_1 y_1'(\nu_2)/L(\nu_2), \qquad y = y_1(\nu_2) + \nu_1 x_1'(\nu_2)/L(\nu_2). \tag{16}$$

The coordinate lines $\nu_1 = \text{const}$ are located at a distance ν_1 from the contour l. The straight lines $\nu_2 = \text{const}$ are normals to the external contour of the plate.

We determine the ultimate load P_0 from Eq. (15) at the time of motion beginning t_0 and from the condition $\ddot{w}_c(t_0) = 0$. Then, we have

$$P_0 = \frac{M_0(2-\eta)\displaystyle\sum_{i=1,2}\sum_j \int\limits_{l_{ij}} G_{ij}\, dl}{\displaystyle\sum_{i=1,2}\sum_j \iint\limits_{Z_{ij}} G_{ij} d_{ij}\, ds + \iint\limits_{Z_a} ds}. \tag{17}$$

2. We consider the dynamic motion of curved plates with an arbitrary rigid insert by an example of a circular plate with a regular n-angle rigid insert located at the center. Let R and R_1 be the radii of the circular plate and the circumference inscribed into the polygonal contour of the rigid insert, respectively; $R_1 < R\cos(\pi/n)$ (Fig. 4). Under medium loads, the plate is deformed into a line surface with formation (owing to its symmetry) of n identical zones Z_2, i.e., we have scheme No. 1 (see Fig. 4); the velocity of the angle of rotation on the support contour is $\dot{\alpha}_2(t, \varphi)$. Under high loads, n identical zones Z_p are formed in the central part of the plate, in the vicinity of the rigid insert, i.e., we have scheme No. 2 (Fig. 5). Equation (1) for l_3 of the contour Z_p in the polar coordinate system has the form

$$x_3 = (R - D)\cos\varphi, \qquad y_3 = (R - D)\sin\varphi \qquad (-\xi \leqslant \varphi \leqslant \xi, \quad 0 < \xi < \pi/n).$$

There are still n identical zones Z_2: $\xi \leqslant \varphi \leqslant (2\pi/n) - \xi$. Under superhigh loads, there are no zones Z_2, whereas the insert Z_a is located inside the zone Z_p and $D \leqslant R - R_1/\cos(\pi/n)$, i.e., we have scheme No. 3 (Fig. 6).

In this case, the equations of plate motion (7)–(9), (11), and (12) for the scheme of deformation No. 2 are

$$\rho\ddot{\alpha}\Sigma_1 = P(t)\Sigma_2 - M_0(2-\eta)\Sigma_3; \tag{18}$$

$$\ddot{w}_c(\rho\Sigma_4 + \rho_a\Sigma_5) = P(t)\Sigma_6; \tag{19}$$

$$D = R - R_1/\cos\xi; \tag{20}$$

$$\dot{\alpha}_2(t, \varphi) = F_2(t, \varphi)\dot{\alpha}(t); \qquad F_2(t, \varphi) = [R - R_1/\cos\xi(t)]/(R - R_1/\cos\varphi). \tag{21}$$

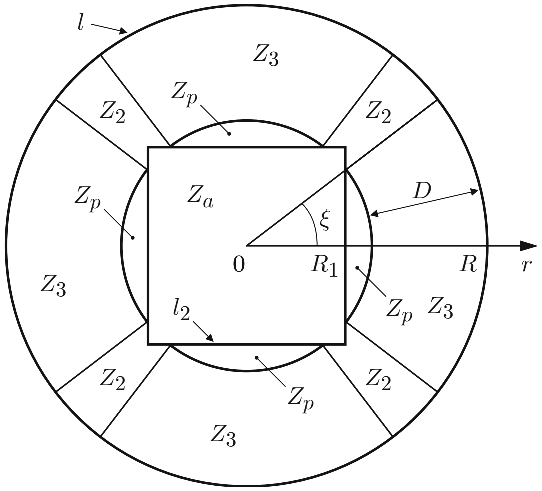

Fig. 5

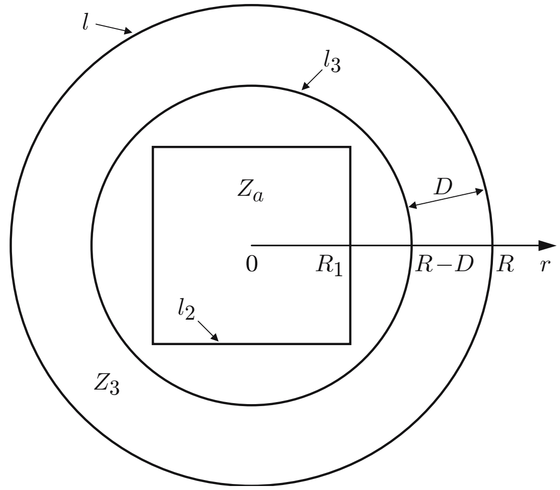

Fig. 6

Here

$$\Sigma_1(\xi) = \frac{n(R\cos\xi - R_1)^2}{6\cos^2\xi}\Big\{\xi\,\frac{(R\cos\xi - R_1)(R\cos\xi + 3R_1)}{\cos^2\xi} + R^2\Big(\frac{\pi}{n} - \xi\Big)$$

$$- 3R_1^2\Big(\tan\frac{\pi}{n} - \tan\xi\Big) + 2RR_1\Big[\ln\frac{\cos(\pi/n)}{1-\sin(\pi/n)} - \ln\frac{\cos\xi}{1-\sin\xi}\Big]\Big\};$$

$$\Sigma_2(\xi) = \frac{n(R\cos\xi - R_1)}{3\cos\xi}\Big\{\xi\,\frac{(R\cos\xi - R_1)(R\cos\xi + 2R_1)}{\cos^2\xi} + R^2\Big(\frac{\pi}{n} - \xi\Big)$$

$$+ RR_1\Big[\ln\frac{\cos(\pi/n)}{1-\sin(\pi/n)} - \ln\frac{\cos\xi}{1-\sin\xi}\Big] - 2R_1^2\Big(\tan\frac{\pi}{n} - \tan\xi\Big)\Big\};$$

$$\Sigma_3(\xi) = 2nR\Big[\xi + \frac{R\cos\xi - R_1}{R\cos\xi}\Big(\frac{\pi}{n} - \xi + \frac{R_1}{A_*}\Sigma_*\Big)\Big]; \qquad \Sigma_4(\xi) = nR_1^2\Big(\frac{\xi}{\cos^2\xi} - \tan\xi\Big);$$

$$\Sigma_5 = nR_1^2\tan\frac{\pi}{n}; \qquad \Sigma_6(\xi) = \Sigma_4(\xi) + \Sigma_5 = nR_1^2\Big(\frac{\xi}{\cos^2\xi} - \tan\xi + \tan\frac{\pi}{n}\Big);$$

$$\Sigma_* = \ln\frac{[B_*\tan(\pi/2n) + A_*][-B_*\tan(\xi/2) + A_*]}{[-B_*\tan(\pi/2n) + A_*][B_*\tan(\xi/2) + A_*]}; \qquad B_* = R + R_1; \qquad A_* = \sqrt{R^2 - R_1^2}.$$

Then, the plate motion by scheme No. 2 is described by Eqs. (10) and (18)–(21).

The equations of the plate motion (14) and (15) by scheme No. 1 have the form

$$\dot\alpha_2(t,\varphi) = G_2(\varphi)\dot w_c(t); \qquad G_2(\varphi) = \cos\varphi/(R\cos\varphi - R_1); \tag{22}$$

$$\ddot w_c(\rho\Sigma_7 + \rho_a\Sigma_5) = P(t)\Sigma_8 - M_0(2-\eta)\Sigma_9, \tag{23}$$

where

$$\Sigma_7 = \Sigma_1(0)/(R - R_1)^2; \qquad \Sigma_8 = \Sigma_2(0)/(R - R_1) + \Sigma_5; \qquad \Sigma_9 = \Sigma_3(0)/(R - R_1).$$

The equations of the plate motion (8) and (9) by scheme No. 3 have the form

$$\rho\ddot\alpha\Sigma_{10} = P(t)\Sigma_{11} - M_0(2-\eta)\Sigma_{12}; \tag{24}$$

$$\ddot w_c(\rho\Sigma_{13} + \rho_a\Sigma_5) = P(t)\Sigma_{14}. \tag{25}$$

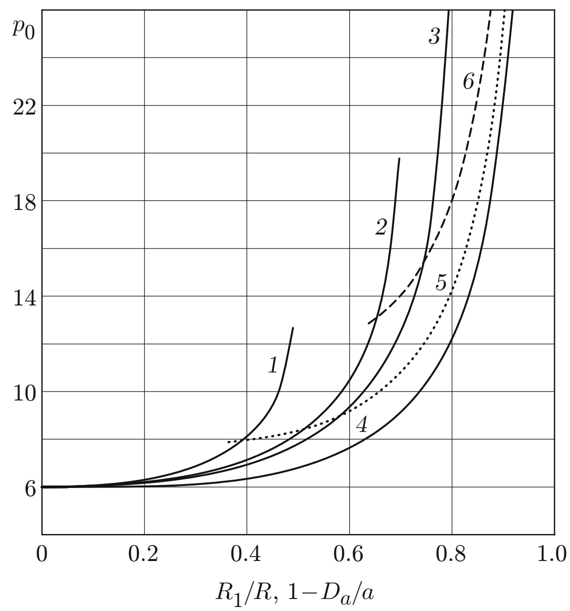

Fig. 7

Here

$$\Sigma_{10}(D) = D^3(4R - 3D)/6; \quad \Sigma_{11}(D) = D^2(3R - 2D)/3; \quad \Sigma_{12} = \Sigma_3(\pi/n)/\pi = 2R;$$

$$\Sigma_{13}(D) = \pi(R - D)^2 - nR_1^2 \tan(\pi/n); \quad \Sigma_{14}(D) = \Sigma_{13}(D) + \Sigma_5 = \pi(R - D)^2.$$

Then, the plate motion by scheme No. 3 is described by Eqs. (10), (24), and (25).

The ultimate load P_0 (17) is determined as

$$P_0 = \frac{M_0(2-\eta)\Sigma_9}{\Sigma_8} = \frac{M_0(2-\eta)\Sigma_3(0)}{\Sigma_2(0) + (R - R_1)\Sigma_5}. \tag{26}$$

For $R_1 = 0$, the plate considered becomes circular and does not contain any insert. For this case, Eq. (26) yields $P_0 = 6M_0(2-\eta)/R^2$. If the plate is simply supported, this value equals the ultimate load $\bar{P}_0$ obtained in [16] on the basis of the exact solution. In the case of a clamped contour, the ultimate load predicted by Eq. (26) is $2\bar{P}_0$. In [13], it was obtained as a result of an approximate solution on the basis of Tresca's condition of plasticity and equals $1.875\bar{P}_0$. As $n \to \infty$, we obtain a circular rigid insert. For such a plate, the ultimate load is determined as

$$P_0 = 6M_0(2-\eta)R/(R^3 - R_1^3) \tag{27}$$

and coincides, in the case of a simply supported plate, with the ultimate load obtained on the basis of the exact solution [10]. Figure 7 shows the load $p_0 = P_0R^2/[(2-\eta)M_0]$ as a function of the ratio R_1/R for different values of n: $n = 3$ (curve 1), $n = 4$ (curve 2), $n = 5$ (curve 3), and $n = \infty$ (curve 4).

We optimize the shape of a regular n-angle rigid insert to find the extreme value of the ultimate load of the plate considered under the condition of a constant area of the rigid insert S_a, thickness, method of attachment, and radius of the circular plate. As the area of the rigid insert is $S_a = nR_1^2 \tan(\pi/n)$, Eq. (26) acquires the form

$$P_0 = 6M_0(2-\eta)A_1/R^2,$$

$$A_1 = \frac{\dfrac{\pi}{n} + \dfrac{\delta}{1-\delta^2} \ln \dfrac{(1+\delta)\tan(\pi/2n) + \sqrt{1-\delta^2}}{-(1+\delta)\tan(\pi/2n) + \sqrt{1-\delta^2}}}{\pi/n + \delta^2 \tan(\pi/n) + \delta \ln\{\cos(\pi/n)/[1 - \sin(\pi/n)]\}}, \qquad \delta = \frac{1}{R}\sqrt{\frac{S_a}{n\tan(\pi/n)}}.$$

As A_1 decreases with increasing n and the inequality $R_1 = \sqrt{S_a/[n\tan(\pi/n)]} < R\cos(\pi/n)$ has to be satisfied, a circular plate with a circular rigid insert has the minimum ultimate load $P_0 = 6M_0(2-\eta)R/[R^3 - (\sqrt{S_a/\pi}\,)^3]$, and the plate with an n_0-angle rigid insert has the maximum ultimate load [n_0 is the minimum number among all values of n that satisfy the inequality $\sin(2\pi/n)n/2 > S_a/R^2$].

We analyze the plate motion considered with different levels of the explosive load.

1. For $0 < P_{\max} \leqslant P_0$ (low loads), the plate remains at rest.

2. For $P_0 < P_{\max} \leqslant P_1$ (medium loads), where P_1 is the load corresponding to the emergence of the zone Z_p, the plate motion follows scheme No. 1. We determine the load P_1 as follows. Differentiating Eq. (10) in time and eliminating the quantities $\ddot{\alpha}$ and $\ddot{w}_c$ from the resultant equality with the use of Eqs. (18) and (19), we obtain the equality

$$\frac{-\rho\dot{\alpha}\dot{D}}{D}\,\Sigma_1 = P(t)\Big[\Sigma_2 - \frac{\rho\Sigma_1\Sigma_6}{D(\rho\Sigma_4 + \rho_a\Sigma_5)}\Big] - M_0(2-\eta)\Sigma_3. \tag{28}$$

Taking into account that $\dot{\alpha}(t_0) = 0$ and that the equalities $P_1 = P(t_0)$, $D(t_0) = \max D = R - R_1$, and $\xi(t_0) = 0$ are hold if the zone Z_p appears, whereas the zones Z_p and Z_3 are absent, we obtain

$$P_1 = \frac{M_0(2-\eta)\Sigma_3(0)}{\Sigma_2(0) - \rho\Sigma_1(0)\Sigma_6(0)/\{(R-R_1)[\rho\Sigma_4(0) + \rho_a\Sigma_5]\}}. \tag{29}$$

It is seen from Eqs. (26) and (29) that $P_0 < P_1$. We write Eq. (23) for scheme No. 1 in the form

$$\ddot{w}_c(t) = Q[P(t) - P_0], \tag{30}$$

where $Q = \Sigma_8/(\rho\Sigma_7 + \rho_a\Sigma_5)$. The initial conditions have the form (13). At the time $t = T$, the load is removed, and the plate moves by inertia for a certain time.

For $t_0 \leqslant t \leqslant T$, integrating the equation of motion (30), we have

$$\dot{w}_c(t) = Q\Big[\int\limits_{t_0}^{t} P(\tau)\,d\tau - P_0(t-t_0)\Big], \qquad w_c(t) = Q\Big[\int\limits_{t_0}^{t}\int\limits_{t_0}^{m} P(\tau)\,d\tau\,dm - P_0\,\frac{(t-t_0)^2}{2}\Big].$$

For $T < t \leqslant t_f$, the plate motion occurs owing to inertia until the plate stops at the time t_f; it is described by the equation

$$\ddot{w}_c(t) = -QP_0$$

with the initial conditions $\dot{w}_c(T)$ and $w_c(T)$. The time t_f is determined by the condition

$$\dot{w}_c(t_f) = 0. \tag{31}$$

Integrating the equation of motion, we obtain the equalities

$$\dot{w}_c(t) = \dot{w}_c(T) - QP_0(t-T); \tag{32}$$

$$w_c(t) = w_c(T) + \dot{w}_c(T)(t-T) - QP_0(t-T)^2/2.$$

It follows from Eqs. (31) and (32) that

$$t_f = t_0 + \frac{1}{P_0}\int\limits_{t_0}^{T} P(t)\,dt. \tag{33}$$

The deflections are calculated by Eqs. (4) and (22), and the maximum final flexure is found by the formula

$$w_c(t_f) = Q\Big[\frac{1}{2P_0}\Big(\int\limits_{t_0}^{T} P(t)\,dt\Big)^2 - \int\limits_{t_0}^{T} (t-t_0)P(t)\,dt\Big].$$

3. For high loads $P_1 < P_{\max} \leqslant P_2$ (P_2 is the load at which the zone Z_2 disappears,) the plate motion starts with a developed zone Z_p and $R - R_1/\cos(\pi/n) < D(t_0) \leqslant R - R_1$. The initial values $\xi_0 = \xi(t_0)$ and $D_0 = D(t_0)$ are determined from Eq. (28) with allowance for the equality $\dot{\alpha}(t_0) = 0$ and relation (20):

$$P_{\max}\Big\{\Sigma_2(\xi_0) - \frac{\rho\Sigma_1(\xi_0)\Sigma_6(\xi_0)}{D_0[\rho\Sigma_4(\xi_0) + \rho_a\Sigma_5]}\Big\} = M_0(2-\eta)\Sigma_3(\xi_0). \tag{34}$$

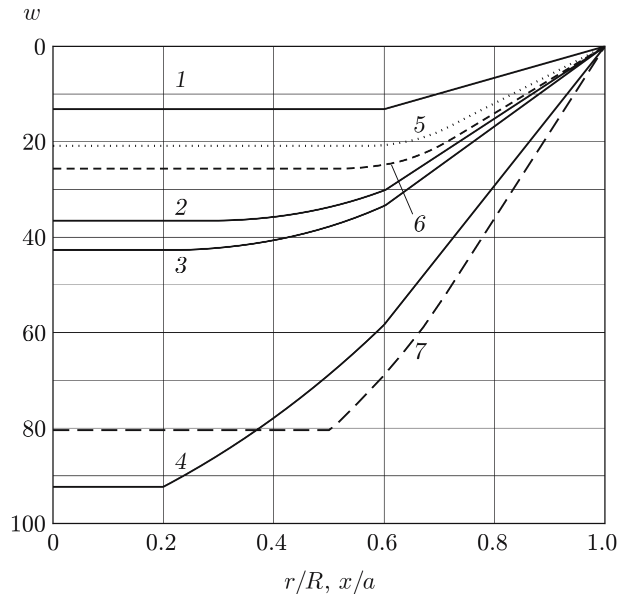

Fig. 8

The load P_2 is determined from equality (34) with $\xi_0 = \pi/n$ and $D_0 = R - R_1/\cos(\pi/n)$:

$$P_2 = \frac{M_0(2-\eta)\Sigma_3(\pi/n)}{\Sigma_2(\pi/n) - \rho\Sigma_1(\pi/n)\Sigma_6(\pi/n)/\{[R - R_1/\cos(\pi/n)][\rho\Sigma_4(\pi/n) + \rho_a\Sigma_5]\}}.$$

In the first phase of deformation ($t_0 < t \leqslant t_1$), the plate motion occurs by scheme No. 2. The deformation is described by Eqs. (10) and (18)–(21) with the initial conditions (13) and (34). In this phase, the zone Z_p is compressed ($\dot{D} > 0$) by the law described by Eq. (28). The time t_1 corresponding to disappearance of the zone Z_p is determined from the equality $\xi(t_1) = 0$. At this time, the values of $\dot{w}_c(t_1)$ and $w_c(t_1)$ are determined.

In the second phase of deformation ($t_1 < t \leqslant t_f$), the plate motion occurs by scheme No. 1 until the stop at the time t_f. The deformation is described by Eqs. (22) and (23) with the initial conditions determined at the end of the first phase of motion. The time of the stop is determined by condition (31). All deflections in the plate are calculated by Eqs. (4) and (20)–(22) with allowance for all phases of motion.

4. For $P_{\max} > P_2$ (superhigh loads), the plate motion starts by scheme No. 3 with a developed zone Z_p, which completely covers the rigid insert Z_a, and then we have $0 < D < R - R_1/\cos(\pi/n)$. We find the value of $D_0 = D(t_0)$ as follows. Differentiating Eq. (10) with respect to time and eliminating $\ddot{\alpha}$ and $\ddot{w}_c$ from the resultant equality with the use of Eqs. (24) and (25), we obtain

$$\frac{-\rho\dot{\alpha}\dot{D}}{D}\,\Sigma_{10} = P(t)\Big[\Sigma_{11} - \frac{\rho\Sigma_{14}\Sigma_{10}}{D(\rho\Sigma_{13} + \rho_a\Sigma_5)}\Big] - M_0(2-\eta)\Sigma_{12}. \tag{35}$$

Taking into account that $\dot{\alpha}(t_0) = 0$, we determine D_0 from the equality

$$P_{\max}\Big\{\Sigma_{11}(D_0) - \frac{\rho\Sigma_{14}(D_0)\Sigma_{10}(D_0)}{D_0[\rho\Sigma_{13}(D_0) + \rho_a\Sigma_5]}\Big\} = M_0(2-\eta)\Sigma_{12}. \tag{36}$$

In the first phase of deformation ($t_0 < t \leqslant t_1$), the plate motion occurs by scheme No. 3. The deformation is described by Eqs. (10), (24), and (25) with the initial conditions (13) and (36). In this phase, the zone Z_p is compressed by the law described by Eq. (35). The time t_1 corresponding to the emergence of the zone Z_2 is determined from the equality $D(t_1) = R - R_1/\cos(\pi/n)$. At this time, the values of $\dot{\alpha}(t_1)$ and $\alpha(t_1)$ are found.

In the second ($t_1 < t \leqslant t_2$) and third ($t_2 < t \leqslant t_f$) phases of deformation, the plate motion occurs in the same manner as the first and second stages of deformation under high loads with appropriate initial values.

All deflections are calculated from Eqs. (4) with allowance for all phases of motion. The solid curves in Fig. 8 refer to the deflections $w = uR^2\rho/(M_0T^2)$ with $\varphi = 0$ of a simply supported circular plate with a square

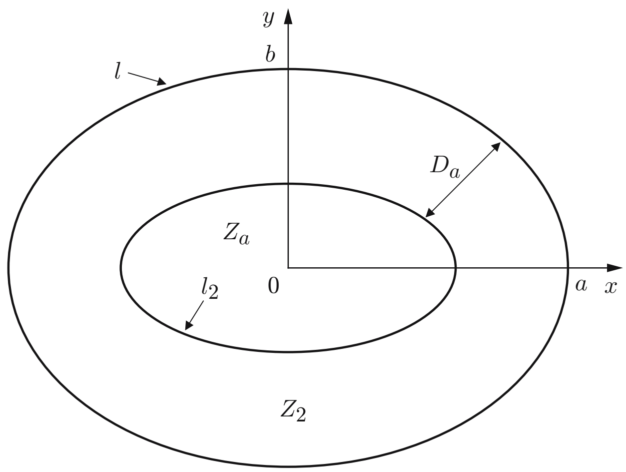

Fig. 9

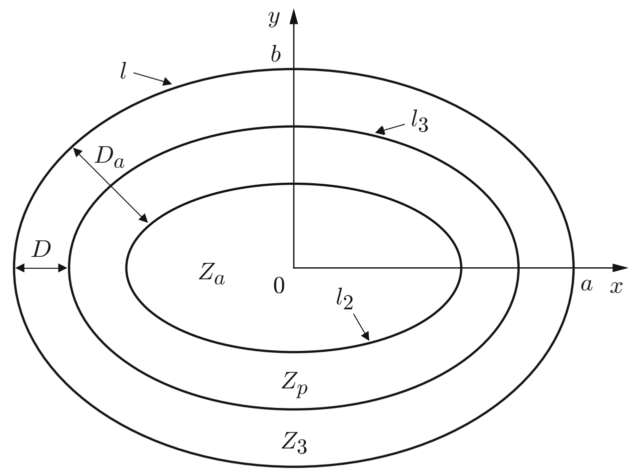

Fig. 10

rigid insert ($n = 4$) and $R_1/R = 0.2$ and $\rho_a/\rho = 3.0$ under the action of a superhigh load of a "rectangular" form: $P(t) = 33.82 M_0/R^2$ (for $0 \leqslant t \leqslant T$) or $P(t) = 0$ (for $t > T$). Curves 1–4 show the deflections of the plate at the times $t = T$, $t = t_1 = 1.89T$, $t = t_2 = 2.12T$, and $t = t_f = 5.88T$, respectively.

3. As another example, we consider the dynamic behavior of an elliptical plate with a rigid insert Z_a whose contour is located at identical distances D_a from the external contour (Fig. 9). The equation of the contour l is set in a parametric form: $x_1 = a\cos\varphi$, $y_1 = b\sin\varphi$ ($0 \leqslant \varphi \leqslant 2\pi$ and $b \leqslant a$). We assume that $0 < D_a \leqslant b^2/a$ and the pivot l_1 is not formed (see [6]). Then, the equation of the contour of the rigid insert l_2 has the form (1) for $D = D_a$. The curvilinear coordinate system (16) has the form

$$x = [a - \nu_1 b/L(\nu_2)]\cos\nu_2, \qquad y = [b - \nu_1 a/L(\nu_2)]\sin\nu_2,$$

$$L(\varphi) = \sqrt{a^2\sin^2\varphi + b^2\cos^2\varphi}.$$

Two deformation schemes are possible for the plate considered. Under medium loads, the plate is deformed in a cone-shaped manner (scheme No. 1; Fig. 9). The angle of rotation of the plate around the support contour of the plate is identical for all φ and equal to $\alpha(t)$. Under high loads, the rigid insert Z_a is located inside the plastic region Z_p, and the contour l_3 is located at identical distances $D_a - D$ from the points of the contour of the rigid insert l_2 (scheme 3; Fig. 10).

The equations of motion (8) and (9) under high loads have the form of Eqs. (18) and (19), where Σ_i should be replaced by Ω_i ($i = 1, \ldots, 6$):

$$\Omega_1(D) = \iint\limits_{Z_3} d_3^2\, ds = \int\limits_0^{2\pi} \Big\{ \int\limits_0^{D} \nu_1^2 \Big[L(\nu_2) - \frac{\nu_1 ab}{L^2(\nu_2)}\Big]\, d\nu_1 \Big\}\, d\nu_2 = \frac{D^3}{6}\Big[8 \int\limits_0^{\pi/2} L(\varphi)\, d\varphi - 3\pi D\Big],$$

$$\Omega_2(D) = \iint\limits_{Z_3} d_3\, ds = \int\limits_0^{2\pi} \Big\{ \int\limits_0^{D} \nu_1 \Big[L(\nu_2) - \frac{\nu_1 ab}{L^2(\nu_2)}\Big] d\nu_1 \Big\} d\nu_2 = \frac{2D^2}{3}\Big[3 \int\limits_0^{\pi/2} L(\varphi)\, d\varphi - \pi D\Big],$$

$$\Omega_3 = \int\limits_l dl = 4 \int\limits_0^{\pi/2} L(\varphi)\, d\varphi; \qquad \Omega_4(D) = \iint\limits_{Z_p} ds = 4(D_a - D) \int\limits_0^{\pi/2} L(\varphi)\, d\varphi - \pi(D_a^2 - D^2),$$

$$\Omega_5 = \iint\limits_{Z_a} ds = \pi ab - D_a\Big[4 \int\limits_0^{\pi/2} L(\varphi)\, d\varphi - \pi D_a\Big],$$

$$\Omega_6(D) = \Omega_4(D) + \Omega_5 = \pi ab - D\Big[4\int\limits_0^{\pi/2} L(\varphi)\,d\varphi - \pi D\Big].$$

Here $d_3(x,y)$ is the distance from the point (x,y) to the support contour; $Z_3 = S \setminus (Z_a \cup Z_p)$. Then, the plate motion is described by Eqs. (10), (18), and (19) with allowance for the replacement made.

The equations of motion (14) and (15) under medium loads have the form

$$\dot{\alpha} D_a = \dot{w}_c; \qquad \ddot{w}_c\Big[\rho\,\frac{\Omega_1(D_a)}{D_a^2} + \rho_a\Omega_5\Big] = P(t)\Big[\frac{\Omega_2(D_a)}{D_a} + \Omega_5\Big] - M_0(2-\eta)\,\frac{\Omega_3}{D_a}.$$

The ultimate load (17) with allowance for $\displaystyle\int\limits_0^{\pi/2} L(\varphi)\,d\varphi \approx \frac{\pi}{8}\,[3(a+b) - 2\sqrt{ab}\,]$ (see [6]) is calculated by the formula

$$P_0 = \frac{M_0(2-\eta)\Omega_3}{\Omega_2(D_a) + D_a\Omega_5} \approx \frac{6M_0(2-\eta)[3(a+b) - 2\sqrt{ab}\,]}{D_a\{4(3ab + D_a^2) - 3D_a[3(a+b) - 2\sqrt{ab}\,]\}};$$

in the case of a circular plate with a circular rigid insert ($a = b = R$ and $D_a = R - R_1$), it coincides with Eq. (27).

An analysis of the dynamic behavior of the plate considered is similar to the analysis performed above for a circular plate with a regular polygonal rigid insert. The difference is that $P_1 = P_2$ and scheme No. 1 is realized after scheme No. 3 for $P_{\max} > P_1$. The load P_1 is calculated by the formula [see Eq. (29)]

$$P_1 = \frac{M_0(2-\eta)\Omega_3}{\Omega_2(D_a) - \dfrac{\rho\Omega_1(D_a)\Omega_6(D_a)}{D_a[\rho\Omega_4(D_a) + \rho_a\Omega_5]}} \approx \frac{6M_0(2-\eta)\rho_a[3(a+b) - 2\sqrt{ab}\,]}{\rho D_a^2[3(a+b) - 2\sqrt{ab} - 2D_a(4\rho_a/\rho - 3)]}.$$

The load $p_0 = P_0 a^2/[(2-\eta)M_0]$ as a function of the ratio D_a/a for different values of b/a is plotted in Fig. 7: curve 4 refers to $b = a$, curve 5 refers to $b/a = 0.8$, and curve 6 refers to $b/a = 0.6$. The dashed and dotted curves in Fig. 8 correspond to the deflections $w = ua^2\rho/(M_0T^2)$ in the cross section $y = 0$ of a simply supported elliptic plate with $b/a = 0.8$, with a rigid insert and $D_a/a = 0.5$, $\rho_a/\rho = 1.5$ under the action of a high load with linear attenuation: $P(t) = 75.48(T - t)M_0/R^2$ for $0 \leqslant t \leqslant T$ and $P(t) = 0$ for $t > T$. Curves 5–7 show the deflections of the plate at the times $t = T$, $t = t_1 = 1.16T$, and $t = t_f = 4.6T$, respectively.

This work was supported by the Russian Foundation for Basic Research (Grant No. 05-01-00161-a).

REFERENCES

1. K. L. Komarov and Yu. V. Nemirovsky, *Dynamics of Rigid-Plastic Structural Elements* [in Russian], Nauka, Novosibirsk (1984).
2. Yu. V. Nemirovsky and T. P. Romanova, “Dynamic behavior of doubly-connected polygonal plastic plates,” *Prikl. Mekh.*, **23**, No. 5, 53–59 (1987).
3. Yu. V. Nemirovsky and T. P. Romanova, “Dynamic bending of polygonal plastic slabs,” *J. Appl. Mech. Tech. Phys.*, **29**, No. 4, 591–597 (1988).
4. Yu. V. Nemirovsky and T. P. Romanova, “Dynamics of plastic deformation of plates with a curvilinear contour,” *Prikl. Mekh.*, **37**, No. 12, 68–78 (2001).
5. Yu. V. Nemirovsky and T. P. Romanova, “Plastic deformation of doubly connected plates with a curvilinear contour under dynamic loads,” in: *Urgent Problems of Dynamics and Strength in Theoretical and Applied Mechanics* [in Russian], Tekhnoprint, Minsk (2001), pp. 515–525.
6. Yu. V. Nemirovsky and T. P. Romanova, “Dynamic plastic damage of simply and doubly connected elliptic plates,” *J. Appl. Mech. Tech. Phys.*, **43**, No. 2, 291–301 (2002).
7. Yu. V. Nemirovsky and T. P. Romanova, “Modeling and analysis of forging of thin-walled structures with smooth convex contours,” in: *Mechanics of Shells and Plates*, Proc. of the XX Int. Conf. on the Theory of Shells and Plates [in Russian], Izd. Nizhegorod. Univ., Nizhnii Novgorod (2002), pp. 231–239.
8. Yu. V. Nemirovsky and T. P. Romanova, “Damage of plane targets with non-concave contours under explosive loading,” *Nauch. Vestn. Novosib. Tekh. Univ.*, No. 2, 77–85 (2002).

9. Yu. V. Nemirovsky and T. P. Romanova, "Dynamic behavior of rigid-plastic plates in the form of a sector," *Prikl. Mekh.*, **40**, No. 4, 93–101 (2004).
10. V. N. Mazalov and Yu. V. Nemirovsky, "Dynamics of thin-walled plastic structures," in: *Dynamic Problems of Plastic Media* (Ser. *News in Foreign Science. Mechanics*) [Russian translation], Issue No. 5, Mir, Moscow (1975), pp. 155–247.
11. M. I. Erkhov, *Theory of Ideal Plastic Solids and Structures* [in Russian], Nauka, Moscow (1978).
12. H. G. Hopkins and W. Prager, "On the dynamics of plastic circular plates," *Z. Angew. Math. Phys.*, **5**, No. 4, 317–330 (1954).
13. A. L. Florence, "Clamped circular rigid-plastic plates under blast loading," *Trans. ASME*, Ser. E: *J. Appl. Mech.*, **33**, No. 2 (1966).
14. A. L. Florence, "Annular plate under a transverse line pulse," *AIAA J.*, **3**, No. 9, 1726–1733 (1965).
15. A. R. Rzhanitsyn, *Structural Mechanics* [in Russian], Vysshaya Shkola, Moscow (1982).
16. H. G. Hopkins and W. Prager, "The load-carrying capacities of circular plates," *J. Mech. Phys. Solids*, **2**, No. 1, 1–13 (1953).